Electronic Supplementary Information (ESI)

Nanostructured Core-Shell Metal Boride-Oxide as Highly Efficient Electrocatalysts for Photoelectrochemical Water Oxidation

Can Lu,[a] Palani R. Jothi,[b] Thomas Thersleff,[c] Tetyana Budnyak,[c] Anna Rokicinska,[d] Kunio Yubuta,[e] Richard Dronskowski,[a,f] Piotr Kuśtrowski,[d] Boniface P. T. Fokwa[b,*] and Adam Slabon[c,*]

[a] Institute of Inorganic Chemistry, RWTH Aachen University, Landoltweg 1, D-52074 Aachen, Germany.

[b] Department of Chemistry and Center for Catalysis, University of California, Riverside, 92507 California, USA.

[c] Department of Materials and Environmental Chemistry, Stockholm University, Svante Arrhenius väg 16c, 10691 Stockholm, Sweden.

[d] Faculty of Chemistry, Jagiellonian University, Gronostajowa 2, 30-387 Krakow, Poland.

[e] Institute for Materials Research, Tohoku University, Katahira 2-1-1, Sendai 980-8577, Japan

[f] Hoffmann Institute of Advanced Materials, Shenzhen Polytechnic, Liuxian Blvd 7098, 518055 Shenzhen, China.

** Corresponding authors e-mails: adam.slabon@mmk.su.se; bfokwa@ucr.edu*

Contents

1. Experimental Section

Synthesis of cobalt boride (CoB) and iron boride (FeB)

All chemicals were used as received. The CoB and FeB were synthesized by a $Sn/SnCl_2$ redox assisted solid-state method.[1] For the synthesis of CoB, 1 mmol anhydrous $CoCl_2$, 2 mmol B, and 1 mmol Sn powder were mixed together in the glove box and then pressed into pellet. While 1 mmol $FeCl_3$, 2.5 mmol B and 1.5 mmol Sn were used to prepare the pellet for FeB. Each pellet was then sealed in a quartz ampoule, and heated at 800 °C for 8 h with the ramping rate of 2 °C /min. After reaction, dark products were dispersed into ~10% con. HCl, after which the products were washed with deionized water and ethanol in succession for several times. The final CoB and FeB powders were obtained after drying them at 120 °C for 12 h.

Synthesis of Tungsten trioxide (WO_3) photoanodes

The bare WO_3 thin films were hydrothermally grown on fluorine doped tin oxide (FTO) coated glasses (2.2 mm thick, Sigma-Aldrich) by a modified route.[2] Prior to the synthesis, FTO substrates were ultrasonically cleaned in acetone, ethanol, deionized water for 10 min each, and then dried at room temperature. For the synthesis of WO_3 thin films, 5 mL of 0.1 M $Na_2WO_4{\cdot}2H_2O$ solution and 10 mL of 0.1 M $H_2C_2O_4{\cdot}2H_2O$ solution were mixed under vigorous stirring. After stirring for extra 5 min, 10 mL of 1 M HCl was added into the above mixture and kept stirring for 10 min. 6 mL of the mixed solution was transferred to a 20 mL Teflon-lined stainless steel autoclave, where a FTO substrate (3 cm × 1.5 cm) was placed at an angel against the wall with the conducting side facing down. The autoclave was tightly sealed and heated at 180 °C for 2 h, then the FTO glass was cautiously washed and dried. The monoclinic WO_3 thin film grown on FTO substrate could be obtained after annealing the substrate at 550 °C for 1 h.

Loading of CoB or FeB on WO_3 photoanodes

The WO_3/CoB and WO_3/FeB photoanodes were fabricated by drop-casting. 2 mg metal boride powder was ultrasonically dispersed in 10 mL absolute ethanol for 15 min to form a suspension. Then 10 μL of the suspension was drop-casted on the surface of the WO_3 photoanode. By repeating the drop-casting process, the desired amount of the metal boride catalysts could be loaded on the electrodes. The as-prepared electrodes were finally dried in vacuum and then kept in the dark. For comparison, CoB and FeB powders were also drop-casted identically on the bare FTO substrates.

Loading of cobalt borate (Co-B_i) on WO_3 photoanodes

The Co-B_i nanosheet was synthesized by the method reported previously.[3] Typically, 5 mL of 0.5 M $NaBH_4$ solution was added into 100 mL of 0.1 mM $Co(NO_3)_2{\cdot}6H_2O$ solution and maintained at room-temperature for 40 min under vigorous stirring. After reaction, the dark product was collected by centrifuging, washing and drying overnight. For the fabrication of WO_3/Co-B_i photoanodes, Co-B_i powder was ultrasonically dispersed in absolute ethanol (200 μg/mL) and 10 μL of the suspension was drop-casted on the surface of the WO_3 photoanode. The desired amount of Co-B_i catalysts could be loaded on the electrodes by repeating the drop-casting process. After drying in vacuum, the electrodes were kept in dark for further characterization.

Loading of cobalt hydroxide ($Co(OH)_x$) on WO_3 photoanodes

The WO_3/$Co(OH)_x$ photoanodes were obtained by a successive ionic layer adsorption and reaction method.[4] The WO_3 electrodes were successively immersed in 0.05 M $Co(CH_3COO)_2$ aqueous solution, deionized water, 0.1 M NaOH aqueous solution and deionized water each for one minute to finish one cycle of the deposition. By repeating the above cycle for several times, the desired amount of $Co(OH)_x$ catalysts could be loaded on the surface of WO_3 electrodes.

2. **Supplemental Figures, Table and Corresponding Illustration**

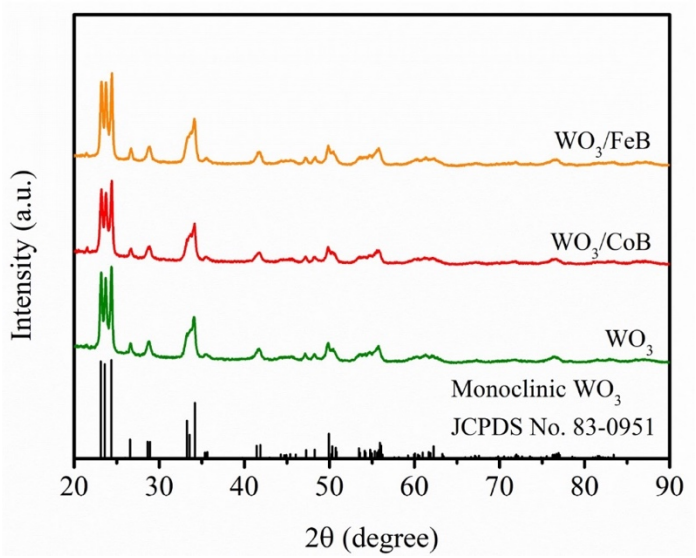

Fig. S1 PXRD patterns of WO_3, WO_3/CoB and WO_3/FeB.

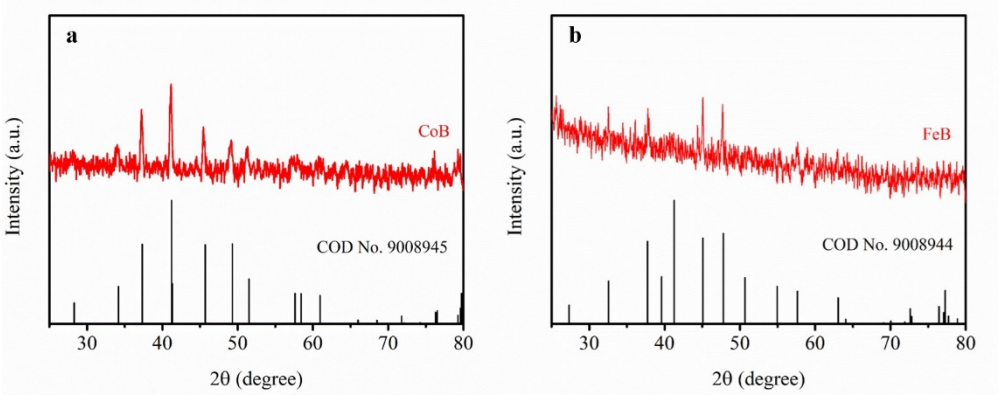

Fig. S2 PXRD patterns of (a) CoB and (b) FeB.

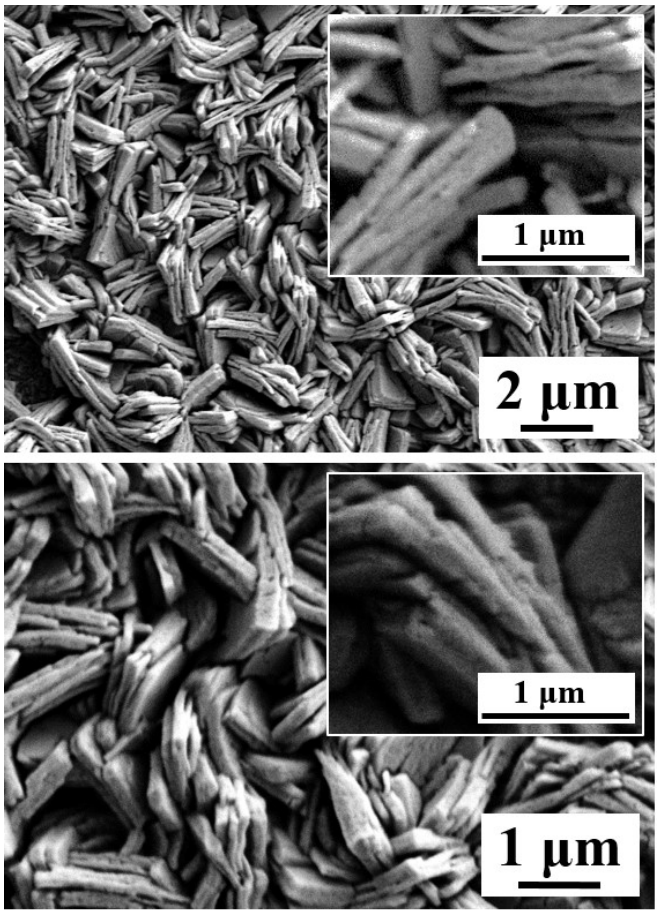

Fig. S3 SEM images of porous sandwich-like WO_3.

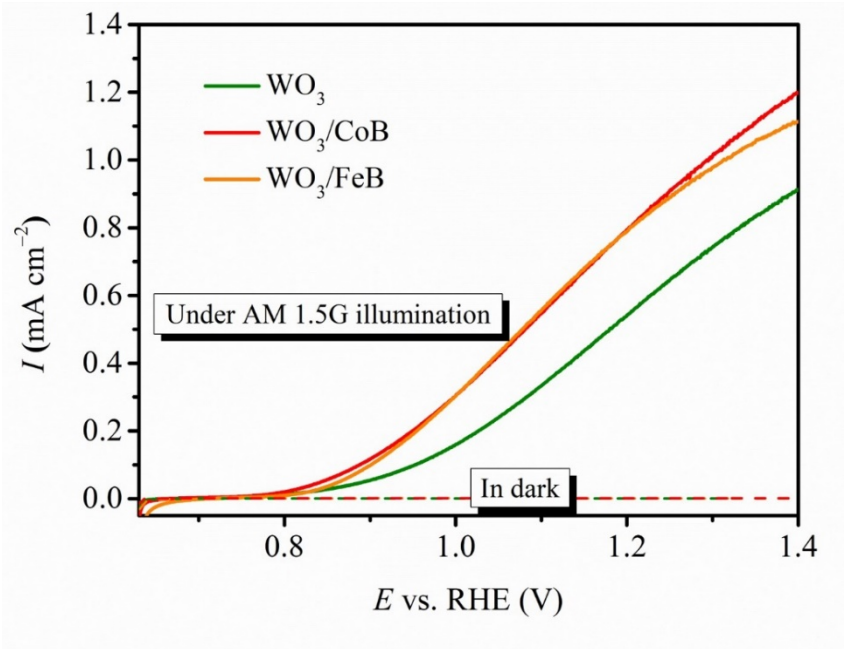

Fig. S4 LSV curves of WO_3, WO_3/CoB and WO_3/FeB electrodes under AM 1.5G illumination or dark in 0.1 M Na_2SO_4 (pH 7).

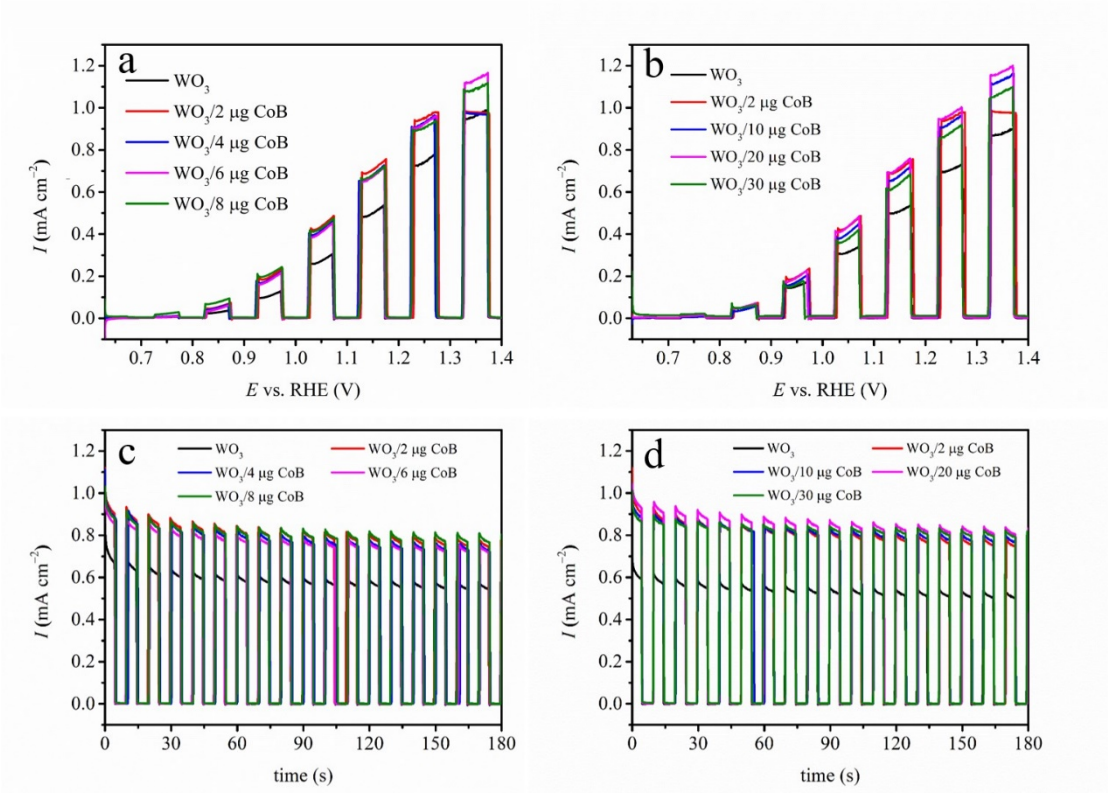

Fig. S5 (a) and (b) LSV curves, (c) and (d) CA curves on the optimization of the loading amount of CoB, recorded under chopped AM 1.5G illumination in 0.1 M Na_2SO_4 (pH 7).

In Fig. S5, the alteration of the loading amount of CoB below 20 μg does not show apparent influence on the photocurrent density. On the basis of cost-effective consideration, 2 μg is chosen for following use.

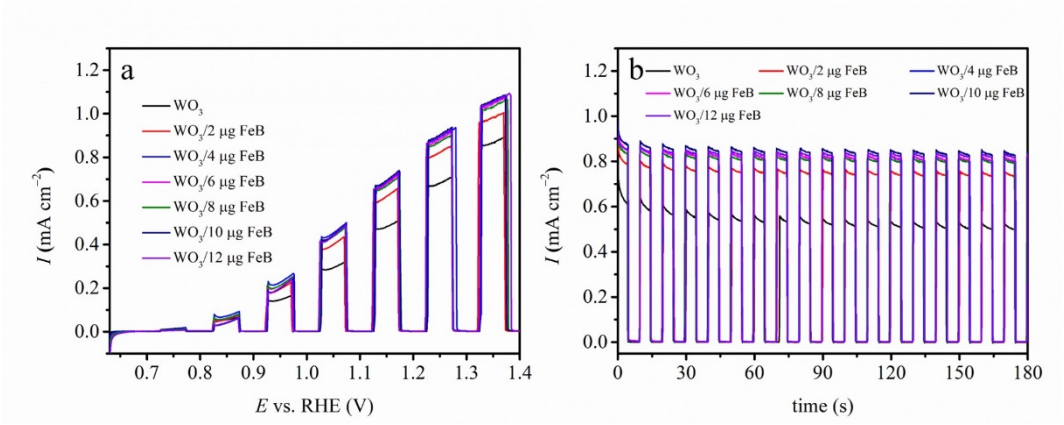

Fig. S6 (a) LSV curves and (b) CA curves on the optimization of the loading amount of FeB, recorded under chopped AM 1.5G illumination in 0.1 M Na_2SO_4 (pH 7).

In Fig. S6, after the loading amount exceeds 4 μg, the alteration of catalyst amount does not show apparent influence on the photocurrent. On the basis of cost-effective consideration, 4 μg is chosen for following use.

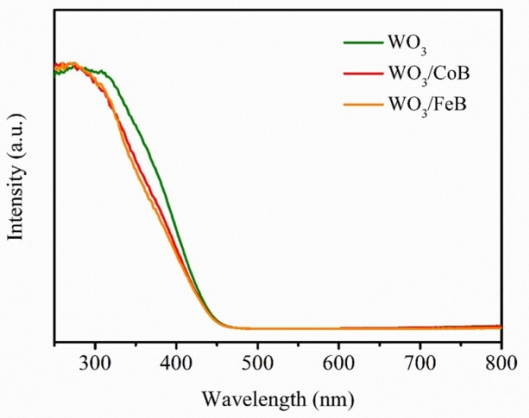

Fig. S7 UV-vis absorption spectra of bare WO_3, WO_3/CoB and WO_3/FeB films.

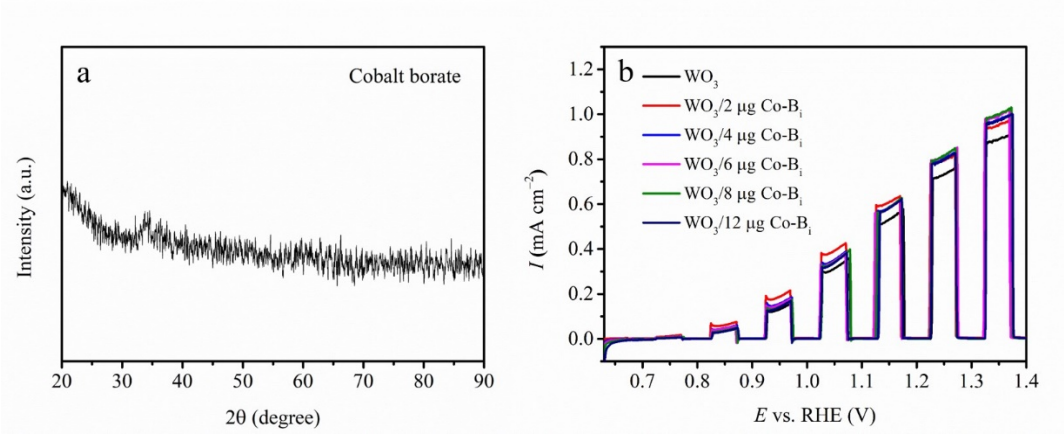

Fig. S8 (a) PXRD pattern of obtained Co-B_i. (b) LSV curves on the optimization of the loading amount of Co-B_i, recorded under chopped AM 1.5G illumination in 0.1 M Na_2SO_4 (pH 7).

In Fig. S8a, the PXRD pattern of Co-B_i reveals that it formed in the amorphous phase, in accordance with the literature.[3] In Fig. S8b, after exceeding the optimal loading amount 2 μg of Co-B_i, the photocurrent get decreased.

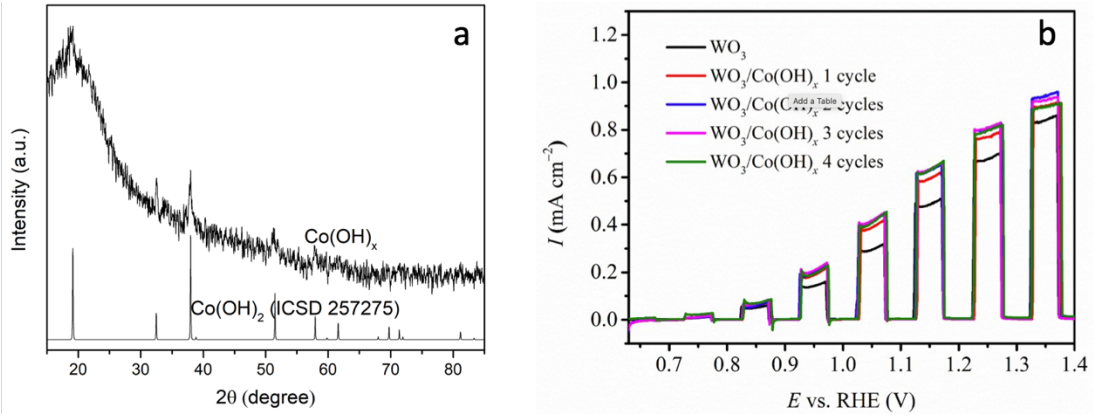

Fig. S9 LSV curves on the optimization of the loading amount of $Co(OH)_x$, recorded under chopped AM 1.5G illumination in 0.1 M Na_2SO_4 (pH 7). By repeating the deposition for 2 cycles, the desired amount of $Co(OH)_x$ catalyst is loaded on the surface of WO_3 electrode.

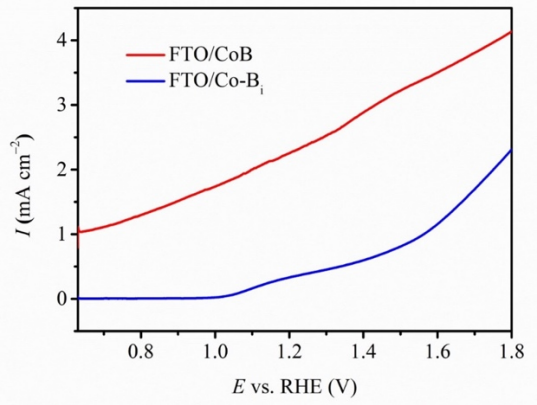

Fig. S10 Dark LSV curves of CoB and Co-B_i electrodes recorded in 0.1 M Na_2SO_4 (pH 7).

To compare the dark oxygen evolution reaction (OER) capacity of the CoB and Co-B_i, 500 mg of the two catalysts were loaded on pure FTO substrates, respectively. After drying in vacuum, the dark LSV scans with the rate of 10 mV/s were performed. Both of the curves in Fig. S10 were recorded from the first scan. It is clear that apparent negative shift of the onset potential and obvious high current are obtained for the CoB electrode, indicating fast OER kinetics on the surface of CoB electrode in comparison with Co-B_i electrode.

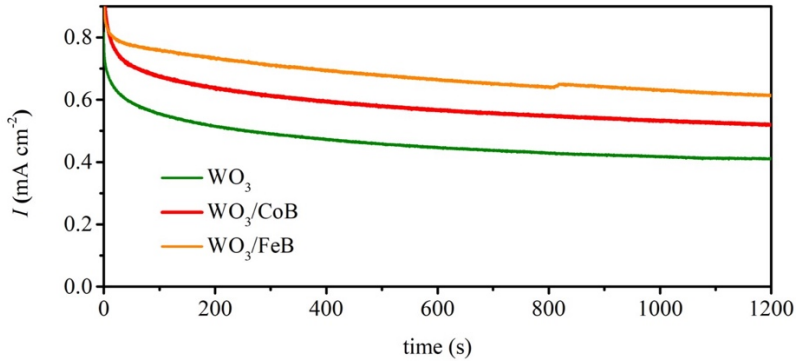

Fig. S11 CA curves of pristine WO_3, WO_3/CoB and WO_3/FeB photoanodes, recorded under AM 1.5 G illumination in 0.1 M Na_2SO_4 electrolyte (pH 7).

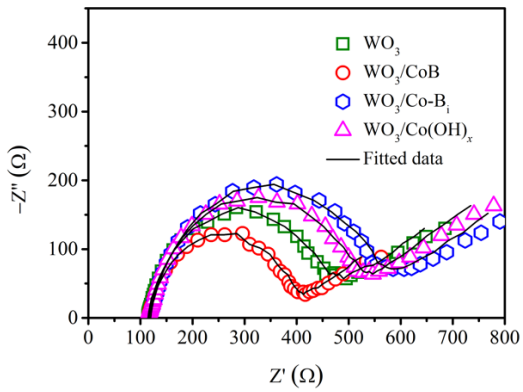

Fig. S12 EIS Nyquist plots with fitted curves of WO_3, WO_3/CoB and WO_3/Co-B_i and WO_3/$Co(OH)_x$ photoanodes at a bias of 1 V_{RHE}, in 0.1 M Na_2SO_4 electrolyte (pH 7) under AM 1.5G illumination.

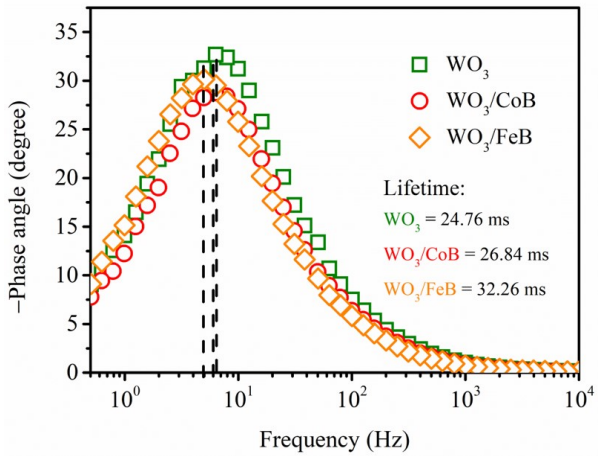

Fig. S13 Bode phase plots of WO_3, WO_3/CoB and WO_3/FeB photoanodes, recorded in 0.1 M Na_2SO_4 electrolyte (pH 7) under AM 1.5G illumination.

Compared to the pristine WO_3 photoanode, the characteristic peaks of modified photoanodes shift to lower frequency, revealing accelerated holes transport and prolonged holes lifetime.[5,6] The lifetime of holes (τ) can be extracted by the following equation:[7]

$$\tau = 1/(2\pi f_m) \quad (1)$$

The τ can be determined by the maximum phase peak in the frequency range (f_m) of bode plots. With respect to the τ of pristine WO_3 photoanode (24.76 ms), the WO_3/CoB and WO_3/FeB photoanodes display prolonged τ of 26.84 and 32.26 ms, respectively. It clearly suggests that integration of CoB and FeB catalysts with the WO_3 photoanodes is prone to facilitate holes transport and charge carrier separation, and thus promoting the photoelectrochemical (PEC) water oxidation.

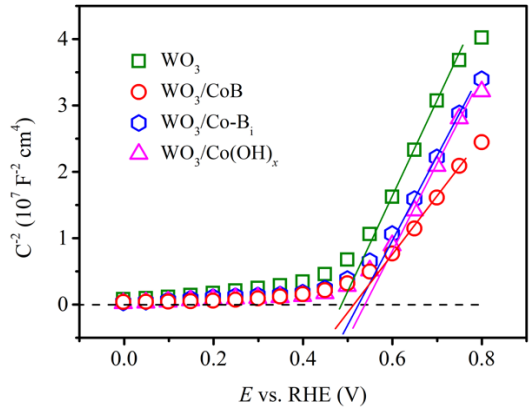

Fig. S14 Electrochemical Mott-Schottky plots of WO_3, WO_3/CoB and WO_3/Co-B_i and WO_3/$Co(OH)_x$ photoanodes at frequency of 10 Hz, recorded in 0.1 M Na_2SO_4 electrolyte (pH 7) under AM 1.5G illumination.

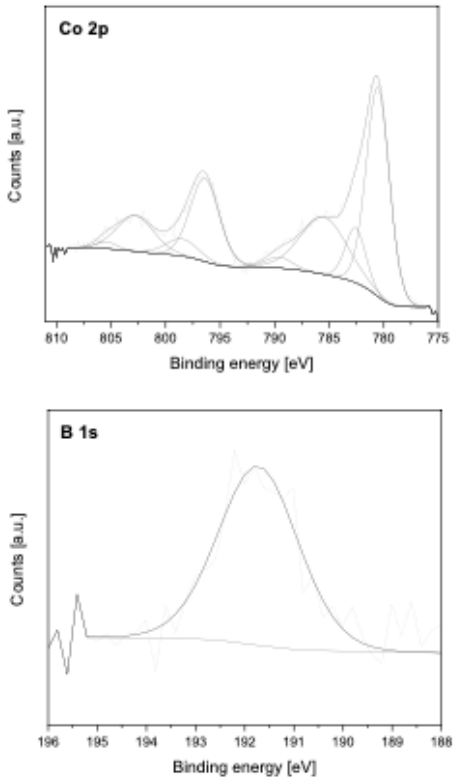

Fig. S15 XP Co 2p and B 1s spectra of CoB electrode after soaking in distilled water for 1 min and drying at 50 °C.

Table S1. Fitting results of resistance elements (R) from Nyquist plots for WO_3, WO_3/CoB and WO_3/FeB photoanodes.

	R_1 (Ω)	R_2 (Ω)	R_3 (Ω)
WO_3	114.7	355.4	281.4
WO_3/CoB	116.3	290.2	166.8
WO_3/FeB	113.8	300.7	144.2

In Table S1, all photoanodes show similar R_1 at around 115 Ω. After coupling CoB and FeB, R_3 diminish apparently. Specifically, R_2 decrease from 355.4 to 290.2 and 300.7 Ω, and R_3 reduce from 281.4 to 166.8 and 144.2 Ω, for WO_3/CoB and WO_3/FeB, respectively. It implies that surface functionalization with CoB and FeB is capable to reduce the resistances for charge carrier transfer, and accelerate holes migration to OER.

Table S2. Fitting results of resistance elements (R) from Nyquist plots for WO_3, WO_3/CoB and WO_3/Co-B_i and WO_3/$Co(OH)_x$ photoanodes.

	R_1 (Ω)	R_2 (Ω)	R_3 (Ω)
WO_3	114.7	355.4	281.4
WO_3/CoB	116.3	290.2	166.8
WO_3/Co-B_i	119.5	462.2	241.3
WO_3/$Co(OH)_x$	116.0	426.5	257.3

In Table S2, all photoanodes show similar R_1. After coupling Co-B_i and Co(OH)$_x$, R_3 diminish while R_2 get increased, suggesting the loading of Co-B_i and Co(OH)$_x$ is mainly prone to mitigate the charge carriers recombination at the electrode/electrolyte interface. Specifically, R_2 upraise from 355.4 to 462.2 and 426.5 Ω, and R_3 reduce from 281.4 to 241.3 and 257.3 Ω, for WO_3/Co-B_i and WO_3/Co(OH)$_x$, respectively. Notably, WO_3 photoanode functionalized with CoB show drastically decreased R_3, if compared to the counterparts. Therefore, the WO_3/CoB photoanode exhibits higher PEC water oxidation capacity than the WO_3/Co-B_i and WO_3/Co(OH)$_x$ photoanodes (Fig. 2).

3. References

1 P. R. Jothi, K. Yubuta and B. P. T. Fokwa, *Adv. Mater.*, 2018, **30**, 1704181.

2 D. Hu, P. Diao, D. Xu and Q. Wu, *Nano Res.*, 2016, **9**, 1735–1751.

3 P. Chen, K. Xu, T. Zhou, Y. Tong, J. Wu, H. Cheng, X. Lu, H. Ding, C. Wu and Y. Xie, *Angew. Chemie Int. Ed.*, 2016, **55**, 2488–2492.

4 C. Zhen, L. Wang, G. Liu, G. Q. (Max) Lu and H. Cheng, *Chem. Commun.*, 2013, **49**, 3019–3021.

5 L. Ma, H. Fan, J. Wang, Y. Zhao, H. Tian and G. Dong, *Appl. Catal. B Environ.*, 2016, **190**, 93–102.

6 L. Ma, H. Fan, M. Li, H. Tian, J. Fang and G. Dong, *J. Mater. Chem. A*, 2015, **3**, 22404–22412.

7 M. Yang, H. He, H. Zhang, X. Zhong, F. Dong, G. Ke, Y. Chen, J. Du and Y. Zhou, *Electrochim. Acta*, 2018, **283**, 871–881.